OPTO-ELECTRONICS REVIEW **8**(4), 426–432 (2000)

Modifications of post-implantation defects and their activity by annealing procedure

Z.T. KUZNICKI*[1], M. LEY[1], and P. HOLLIGER[2]

[1]CNRS, Laboratoire PHASE (UPR 292)
BP 20, 23 rue du Loess, F-67037 Strasbourg CEDEX 2, France
[2]ETI-CEA, Laboratoire d'Electronique, de Technologie et d'Instrumentation
17 rue des Martyrs, F-38054 Grenoble CEDEX 9, France

Photovoltaic characteristics depend simultaneously on optical (absorption, conversion) and electronic (carrier transport and collection) behaviour. We have analysed theoretically and experimentally some possible modifications of the post-implantation defect activity on single-crystal Si in view of a very- and ultra-high photovoltaic conversion efficiency.

Beam-induced structural instabilities that depend on the annealing temperature have been observed for the first time by a spectral response method on heavily doped CZ-Si material. The spectral response results agree well with previous DLTS measurements that can be carried out exclusively on lightly doped material. Modifications of the single-crystal surface layer and its photogeneration activity have been observed after an amorphising dose of ^{31}P beam implantation and related post-implantation thermal treatment.

Important non-linear external quantum efficiency (EQE) transformations can be explained by the oxygen aggregates at post-implantation structural defects. When annealed at the relatively low temperature of 300°C during 40 min or 350°C during 20 min, oxygen will precipitate on defects and form active recombination centres. This phenomenon is reversible because a further annealing at 500°C reduces the recombination activity, probably by dissolution of oxygen clusters. Another annealing at 300°C again activates the recombination centres because the oxygen precipitates once more on non-gettered defects, and so on.

The observed instabilities are coupled with a post-implantation structural gettering and solid phase epitaxy related to the flatness and movements of a-Si/c-Si heterointerfaces.

The possibility of usefulness of defects and traps in solar cells (and especially in implanted Si material) has been investigated since the 1980s. Usually, the conversion efficiency diminishes because of the non-radiative recombination on numerous defects. We show that an adequate implantation and annealing allow an important transformation of conversion, transport, and collection characteristics.

Keywords: beam-induced structural instabilities, oxygen precipitates, post-implantation defects, ion beam amorphisation; recombination activity, planar nanostructure.

1. Introduction

The electronic behaviour of single-crystal silicon devices is strongly influenced by impurities (oxygen, carbon) and intrinsic point defects. In implanted Si material there are not only numerous point defects but also extended defects which can be observed in HREM images [1]. These larger structural defects combined with oxygen can profoundly modify the final optoelectronic performance of implanted solar cells. Oxygen-rich Si crystals show anomalies of type and size of electrical conductivity because of the presence of thermal donors [2].

It has been shown that in classical solar cells with a non-implanted Si material the addition of oxygen into the device bulk improves photovoltaic (PV) performance [3]. The same effect cannot be demonstrated in multi-interface implanted cells. This difference can be explained on the basis of extended defect – oxygen interactions by analogy to the effects observed in polycrystalline silicon in sheet form grown in an inert atmosphere with oxygen added, known as EFG material [4]. It has been shown that oxygen aggregates at structural defects, preferentially at grain boundaries and non-coherent twin bundles. But more interesting for the present study is the fact that the amount of oxygen also varies at dislocations within the grains as a function of annealing conditions. Annealing, even at a very low temperature (350°C), increases oxygen aggregation at structural defects. The electrical effect following that can be quenched by a further annealing at 450°C which seems to cause dissolution of oxygen clusters. The oxygen aggrega-

* e-mail: kuznicki@phase.c-strasbourg.fr

tion or dissolution then provokes a respective consequent increase or decrease of structural defect electrical activity. In general, this activity does not improve the performance of implanted solar cells, but that can be eventually controlled with annealing temperature as mentioned, for example, in Ref. 5.

By analogy, it can be observed that in any material with extended defects the oxygen can be incorporated not only at thermodynamically stable interstitial sites, but also at structural defects [6]. Contrary to the oxygen, present at interstitial sites (quantified only by low temperature IR measurements), the oxygen at the structural defects cannot be quantified. Probably this thermodynamic instability is caused by the nature of oxygen accumulation at structural defects which forms SiO_x clusters, with $x < 2$. These clusters do not have thermal stability of SiO_2 precipitates and their composition seems to depend on the annealing temperature. As has been demonstrated before [7], the oxygen segregation at structural defects strongly affects their electrical activity.

Deep level transient spectroscopy (DLTS) spectra for imperfect crystal structures show differences from those of single crystal Si [4]. This method unfortunately cannot be used in characterisation of all semiconductor materials. In fact, DLTS has been used for simple defects with exponential transients, but in many cases non-exponential transients, caused by high density or multi-level impurities, are observed in less-imperfect crystals like EFG Si.

This work examines modification of the PV performance of single-crystal Si solar cells of a MIND (multi-interface novel device) concept in the presence of extended post-implantation defects and large oxygen concentrations. In particular, post-implantation extended defects can be compared to those of EFG material grain-bulk defects. However, in the latter case, limited doping-impurity concentrations allow related characterisations (e.g. by DLTS) which are totally excluded in the heavily implanted material of MIND solar cells. But by analogy, we can suppose that similar temperature annealings act in the same way in other than EFG Si materials, where the extended defects can be decorated or emptied by oxygen as a function of the annealing temperature. So, as in EFG Si, any imperfect Si crystal contains many deep centres from different level energy states [8,9]. In this approach we neglect, to the first approximation, the oxygen interaction with other defects.

The annealing temperature influences the oxygen incorporation and, as a consequence, its deep level activity observed by spectral response (external quantum efficiency – EQE curves). The modification of oxygen aggregates is directly reflected in the conversion performance because of the variation of the minority carrier recombination velocity.

2. Experiments and results

The solar cells examined for this paper are δ-BSF solar cells of a MIND concept [10-12] produced either with CZ-Si or FZ-Si material. Several types of measurements and treatments have been performed:

- EQE and reflection measurements before a complementary thermal treatment,
- complementary thermal treatment at 500°C during 21 min,
- EQE and reflection measurements after the complementary thermal treatment,
- removal of the rear Al sheet-contact, chemical etching of frosted rear surface and evaporation of a new Al contact,
- EQE and reflection measurements before a contact annealing,
- EQE and reflection measurements after contact annealing,
- SIMS oxygen profile, and
- EQE measurements under a different intensity of incident light.

2.1. IR correction coefficient

The correction coefficient allows comparing the EQE curve shapes of MIND cells obtained at the different stages of measurements. In general, the shapes change after the treatments applied to the samples. Linear and non-linear transformations are observed as a function of wavelength. They are produced either by optical effects (photogeneration, absorption, reflection) or by electronic effects (electronic transport, resistances, potential barriers).

The EQE evolution was always observed after the complementary thermal treatment (CTT) which was applied to improve the inserted substructure activity. This evolution can consist of an important multiplication or division (even more than a factor 10 in some cases). Such a variation definitively masks the effect due to a sub-structure modification which cannot be observed by directly comparing the EQE curve shapes of cells submitted to different treatments.

It is possible to establish a relationship between the curve shapes by selecting a characteristic reference wavelength. The wavelength 1025 nm has been chosen to avoid a possible influence of the front face or the emitter. In these regions the photon absorption is important for the short wavelengths. The corresponding energy (1.21 eV) is sufficient for photogeneration in c-Si.

After a complementary thermal treatment, different variations of the spectral response have been observed from mechanisms having different origins:

- front face (contact, crystalline quality of the superficial region, oxygen),
- emitter (post-implantation defects, oxygen, substructure with its interfaces and its transition zones, electron transport parameters, diffusion length),
- collecting p-n junction (quality coefficient, space charge region),
- base (post-implantation defects, electron transport parameters, diffusion length),
- rear face (BSF, contact).

The variations due to the front face have been minimised because of optimisation of the metal-semiconductor contact specially designed to support a thermal treatment up to 700°C, which has been confirmed by all later characterisations.

In our experiments, the non-linear variation due to the defects and undesired impurities in the emitter, the junction and the base are relatively less important than the variations produced by the rear face. The rear contact was neither specially studied nor carefully deposited. Its behaviour changes spectacularly during the complementary thermal treatment because of the potential barrier that increases with the thermal treatment duration (possibility because of an intermediate oxide layer growing during the CTT). This means that the rear contact can produce a serial resistance rise during the thermal treatment and, consequently, a linear transformation of the EQE curves.

The effect of the serial resistance introduced by the rear contact has been confirmed by the following study:

- comparison of EQE characterisations of the same sample before and after the CTT,
- computation of the correction coefficient at 1025 nm,
- multiplication by the EQE correction coefficient taking into account its smallest value at 1025 nm,
- confirmation of the overlap of the two curves in the IR range, $900 < \lambda < 1200$ nm,
- frequently observed difference of the two curves in the visible and UV,
- removal of the rear contact and the intermediate oxide layer between metal and semiconductor,
- deposition of a new Al sheet contact by evaporation,
- measurement of the spectral response with the new rear contact before its annealing,
- measurement of the spectral response with the new rear contact after its annealing,
- comparison of differences in the UV and visible among the three measured results after the applied CTT,
- computation of correction coefficients,
- comparison of the curve shape obtained after the CTT with the curve shape measured before the CTT,
- overlap of the three curves (multiplied by their corresponding correction coefficients) measured after the CTT is always observed in the IR range,
- conclusion 1: the important EQE transformations after the CTT are due to the metal-semiconductor contact; they are linear in the IR range and correspond to the existence of a serial resistance introduced by the different treatments (CTT, contact annealing),
- conclusion 2: the EQE variations before and after the CTT have different origins, as for example:
  (i) transformation of the substructure activity,
  (ii) modification of contact resistance,
  (iii) defect activation/deactivation,
- in typical solar cells, the non-linear EQE transformations are normally not observed.

The correction coefficient permits comparing the shapes of EQE transformations of the same sample by overcoming the problem of an imperfect rear contact (if the curves overlap even only in the IR range). For example, Fig. 1 shows two EQE curves measured with and without a large series resistance (especially bad rear contact). After multiplying curve 14, which initially was close to the x-axis, by the correction coefficient 408.22 (!) established at 1025 nm, the two curves are identical over the whole spectrum.

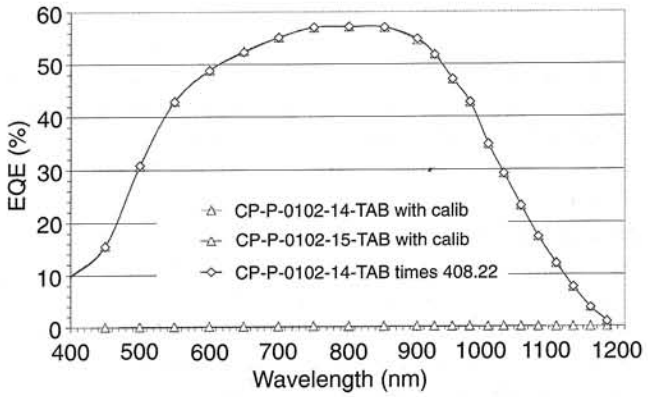

Fig. 1. Comparison of two EQE curves measured with and without a large series resistance (especially bad rear contact for the EQE measurement 14 close to the x-axis) showing the effect of the correction factor. Even the factor of 408 does not influence the form of the linear EQE transformation.

2.2. Spectral response modifications

A comparison of the normalised internal quantum efficiency (IQE) curves of Figs. 2 and 6 allows separation of two concordant effects revealed after the thermal treatment at 500°C, i.e., two simultaneous improvements of:

- solid epitaxy of a-Si/c-Si heterointerfaces,
- quenching activity of oxygen centres. Figure 2 shows the normalised spectral response curves after an initial thermal treatment at 500°C for 21 min and a complementary thermal treatment of the same duration at the same temperature.

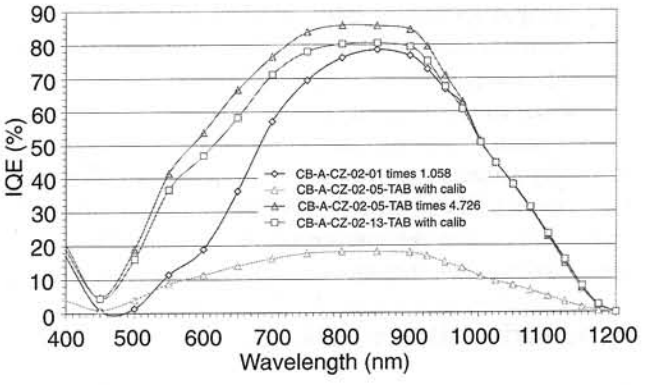

Fig. 2. Comparison of three IQE curves measured on the same CB-A-CZ-02 sample before and after a complementary thermal treatment (CTT) at 500°C for 21 min. Measurement: 01 – before CTT with the first rear contact, 05 – after.

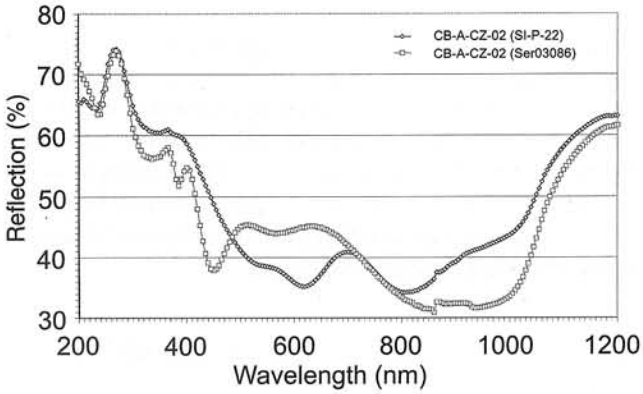

Fig. 3. Comparison of two reflection curves measured before and after a complementary thermal treatment as in Fig 2.

Figure 3 shows the reflection measurements before and after the CTT which confirm an important non-linear transformation due to the displacement of the a-Si/c-Si heterointerfaces during the CTT.

The fringes in the reflection curves are due to the inference of light reflected from the sample surface with that from the c-Si/a-Si and a-Si/c-Si interfaces. Modification of these fringes could be related to a movement of the c-Si/a-Si interface by solid epitaxy. There are two characteristic modifications:

- in the range 300 nm < λ < 700 nm one depends on the upper c-Si/a-Si heterointerface movement and
- in the range 750 nm < λ < 1200 nm one seems to be linked to the bottom a-Si/c-Si heterointerface movement and improvement.

What is more, the CZ-Si single-crystal material used contains, in the most interesting device surface zone, a very large oxygen concentration as shown in the SIMS profile of Fig. 4. This oxygen can easily interact with numerous post-implantation defects and especially with the extended ones. After the post-implantation thermal treatment, the

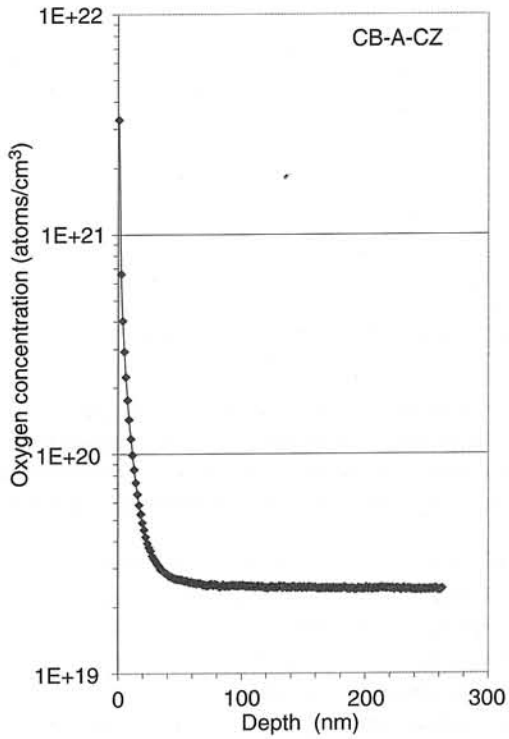

Fig. 4. SIMS profile of the oxygen distribution within the CB-A-CZ sample surface layer. The minimal oxygen concentration at 260 nm is 2.4×10^{19} atoms/cm^3.

point defects disappear [13] and only extended defects remain. This fact is illustrated by a typical contrast in HREM images [1] (Fig. 5). At extremely high annealing temperatures (exceeding 1000°C [13]) extended defects can also be totally gettered, at least from the light absorption point of view.

To be useful for further interpretation, the reported results differentiate combined oxygen and solid phase epitaxy effects revealed at higher temperatures from those caused only by the oxygen (seen at low temperatures).

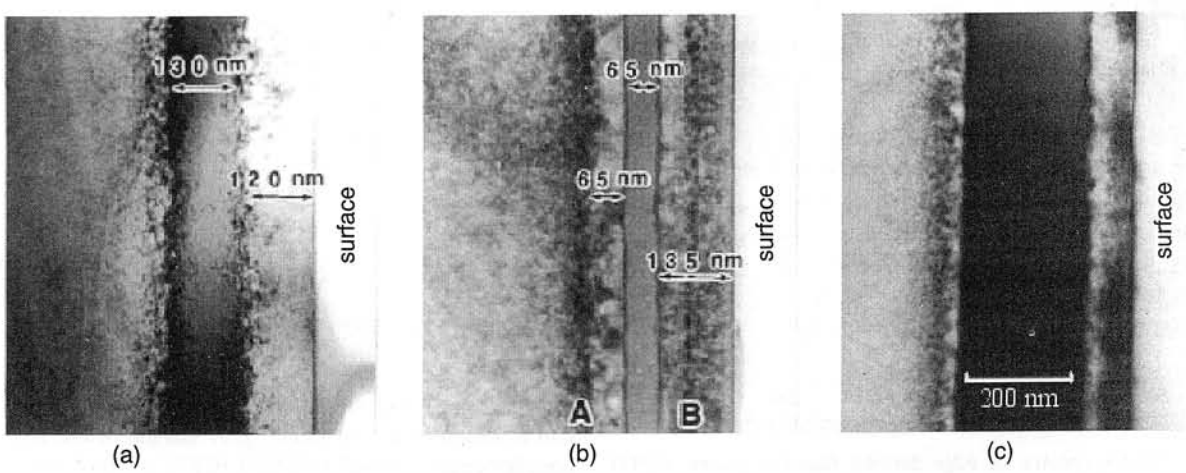

Fig. 5. HREM images of amorphised layers buried by implantation with their crystalline neighborhood: (a) as-implanted, (b) after an adequate thermal treatment, and (c) after a poorly adapted thermal treatment. Dark A and B areas appearing as vertical bands in the central and upper c-Si layer of (b) and the corresponding shadowed area within the bottom c-Si layer of (c) represent extended defects. In the devices with a small oxygen concentration these extended defect zones do not influence the electronic device behaviour (after Ref. 1).

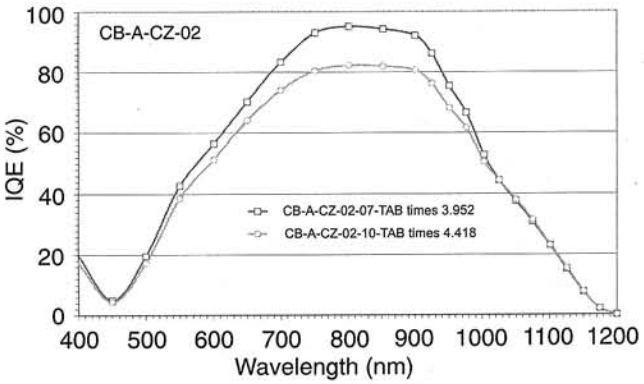

Fig. 6. Same as Fig. 2 but with only two curves: after CTT with the newly non-formed (measurement 07) and formed rear contact (measurement 10). These two curves are normalised to the best result obtained for the same sample at 1025 nm (EQE measurement 13).

Figre 6 shows transformation caused exclusively by the strengthening of the oxygen activity because of an annealing temperature too low to move the a-Si/c-Si heterointerfaces [14]. The most interesting non-linear transformations can be observed between 450 and 1000 nm.

The contact annealing was performed at 300°C for 40 min. These conditions correspond very well to the accumulation of oxygen in the post-implantation extended defects. The characteristic IR part of the normalised IQE curve (between 1000 and 1200 nm) conserves its initial form. However, for shorter wavelengths ($\lambda < 1000$ nm), the deterioration of performance is considerable. It can be explained by a single-crystal bulk transformation, more precisely concerning the electron transport behaviour within the extended defect region. The short-circuit current of spectral response is reduced, most probably by amplified recombination activity (transformation of generation/recombination balance because of the appearance of multi-level energy states) which follows the oxygen accumulation on the extended centres. A corresponding activation/deactivation of oxygen in Si with extended defects has been shown with DLTS measurements [4] (Fig. 7).

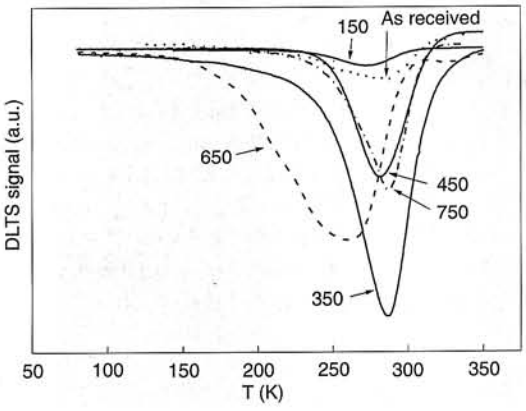

Fig. 7. DLTS spectra of edge-defined film-fed grown (EPG) sample with low oxygen content after annealing at different temperatures [4]. These silicon sheets have large grains and contain numerous structural defects (dislocations, coherent and non-coherent twin bundles, and grain boundaries).

A second complementary thermal treatment at 500°C has been applied to reduce the oxygen activity by dissolution of oxygen clusters. It was limited to 2 min only, because it is wanted that the amorphised substructure persists. Figure 8 shows three reflection measurements indicating the most important modification in the wavelength range between 450 nm and 550 nm. A 500°C thermal treatment of 2 min was enough to give again the reflection measured before the 300°C contact annealing.

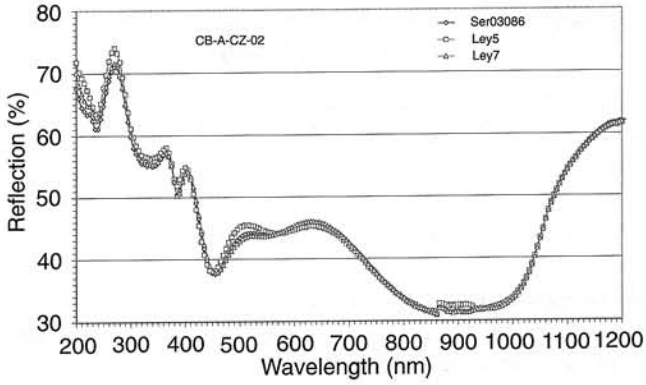

Fig. 8. Comparison of three reflection curves measured before (Ser03086) the contact annealing, after the contact annealing (Ley5) and after the second very short (5 min) complementary thermal treatment at 500°C (Ley7).

After the contact annealing, the reflection changes because of modification of the refractive index due to the formation of oxygen clusters. Even a short second complementary thermal treatment at 500°C is enough to come back to the reflection values before the contact annealing because of the recrystallisation of the heterointerface c-Si transition zone being free of oxygen clusters.

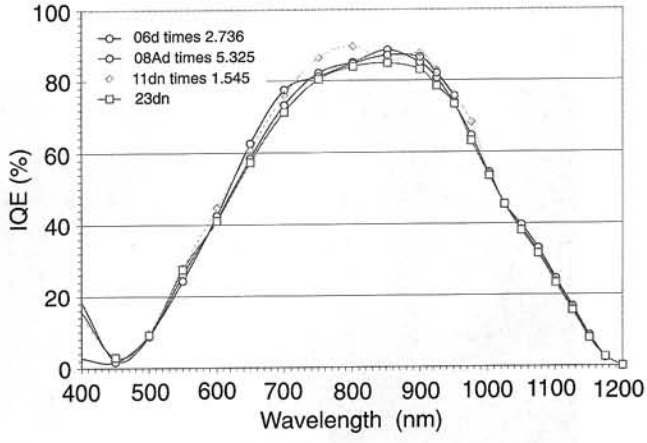

Fig. 9. Comparison of four internal quantum efficiency (IQE) curves measured on the same FZ-07 sample before and after a complementary thermal treatment (CTT) at 500°C for 21 min. Measurement: 06 – before CTT with the first rear contact, 08 – after CTT with the first rear contact, 11 – after CTT with the new rear contact (without contact annealing) and 23 after CTT and contact annealing.

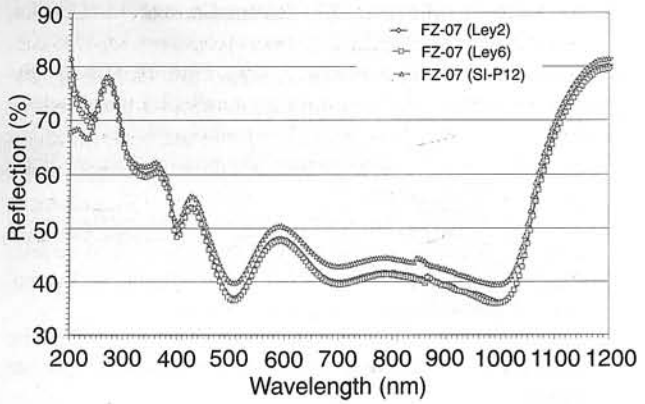

Fig. 10. Comparison of reflection curves measured before the first complementary thermal treatment at 500°C (SI-P12), after the contact annealing (Ley2) and after a second complementary thermal treatment at 500°C (Ley6).

Contrary to the reflection, an equivalent evolution cannot be observed in EQE measurements. Possibly the second CTT was too short to destroy the oxygen clusters and only the displacement of the a-Si/c-Si causes a modification of the reflection

The same measurements have been made for a (δ-BSF solar cell produced with FZ-Si material containing less oxygen than the CZ-Si material, but a similar number of extended defects. Figure 9 shows different IQE results.

The modifications observed after the different thermal treatments are less important than in the case of a solar cell made with a CZ-Si material. This can also be shown with the reflection curves. Figure 10 shows the corresponding reflection measurements on the sample FZ-07. In the case of FZ-Si material it is only the first CTT which changes the reflection of the sample.

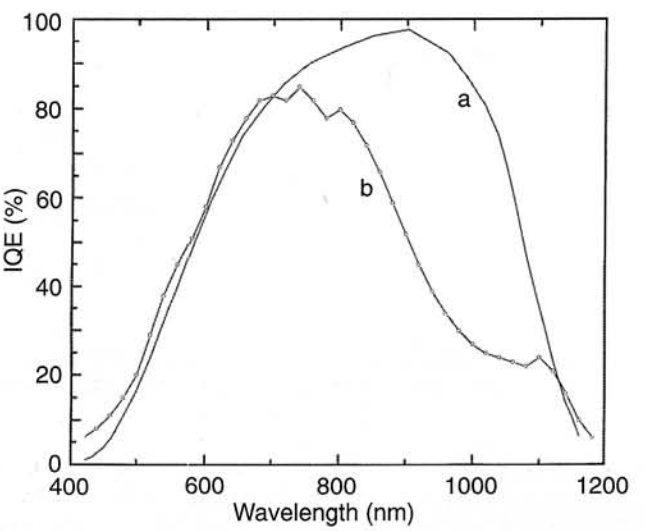

Fig. 11. Comparison of two spectral responses of internal quantum efficiencies (IQE) of the same device measured under two monochromatic light fluxes: curve (a) light intensity about one order of magnitude greater than for curve (b) (after Ref. 15).

On the basis of these results, one can conclude that post-implantation extended defects are not able to modify the spectral response behaviour when the oxygen concentration is relatively small.

The post-implantation defects combined with a high oxygen bulk concentration create a large number of recombination centres in the c-Si upper layer bulk. Their negative effect on the spectral response can be quenched by trap saturation because of the carrier reservoir formed between the sample surface and the c-Si/a-Si heterointerface [15]. This effect is shown in Fig. 11. Two different light intensities have been used: a weak one of the order of μWcm^{-2} and a strong one of hundreds of μWcm^{-2}. For the strong light flux the spectral response has its usual form. For the weak one it is partially quenched by non-saturated traps [15].

3. Conclusions

The oxygen activity in the heavily doped Si crystal seems to be similar to that of the moderately doped as can be measured by the DLTS method [4]. This could be shown with our method using the spectral response, the reflection and a correction coefficient.

The fact that oxygen is present in a relatively large concentration is not necessarily bad for the device, contrary to a conclusion in one of our previous papers [15]. It depends on the temperature of the isothermal annealing, 300°C (O activation) and 450°C (O deactivation). The correction coefficient method allows the comparison of linear and non-linear transformations. The rear face region interacting with long wavelength light changes the IQE linearly whereas the front face region changes it non-linearly. In this front region, post-implantation defects and a large concentration of oxygen atoms are simultaneously present.

The isothermal CTT at 500°C produces two simultaneous transformations:

- oxygen deactivation,
- substructure recrystallisation,

contrary to the annealing at 300°C which acts only on the oxygen activity.

The comparison of CZ and FZ materials confirms that the role of oxygen is dependent on the annealing conditions. The spectral response for CZ material (with oxygen) varies depending on treatment temperature. This is in opposition to variation of the spectral response for FZ material which is less important because of a smaller oxygen concentration (present only in the surface regions).

Acknowledgements

The authors wish to thank A. Mesli of the PHASE Laboratory and A. Pape of the Institute of Subatomic Research of Strasbourg for their comments and C. Weymann for her experimental help.

References

1. Z.T. Kuznicki, J. Thibault, F. Chautain-Matys, and S. Unamuno, "Towards ion beam processed single-crystal Si solar cells with a very high efficiency", *Proc. New Photovoltaics Materials for Solar Cells*, First Polish-Ukrainian Symposium, Cracow-Przegorzały, 99–107 (1996).
2. P. Wagner and J. Hage, "Thermal double donors in silicon", *Appl. Phys* A **49**, 123–138 (1989).
3. B.R. Bathey, R.O. Bell, J.P. Kalejs, M. Prince, M.D. Rosenblum, R.W. Stromont, and F.V. Wald, *Proc. 11th E.C. Photovolt. Sol. En. Conf.*, Montreux, 462 (1992).
4. V. Borjanovic, I. Kovacevic, B. Santic, and B. Pivac, "Oxygen-related deep levels in oxygen doped EFG poly-Si", *Proc. E-MRS, Symposium*, Strasbourg, F–II/P26 (1999).
5. C. Hässler, J. Libermann, S. Thurm, and W. Koch, "Lifetime improvement in multicrystalline silicon: identification and dissociation of thermal oxygen donors", *14th European Photovoltaic Solar Energy Conference*, Barcelona, 720–723 (1997).
6. B. Pivac, A. Sassalla, and A. Borghesi, *Microchim. Acta* **14**, 485 (1997).
7. S. Acerboni, S. Pizzini, S. Binetti, M. Acciari, and B. Pichaud, *J. Appl. Phys.* **76**, 2703 (1994).
8. Y. Yang, S. Mil'stein, J.T. Borenstein, and J.I. Hanoka, *Appl. Phys. Lett.* **56**, 2222 (1990).
9. S.H. Park and D.K. Schroder, *J. Appl. Phys.* **78**, 801 (1995).
10. Z.T. Kuznicki, "Multiinterface solar cells: I. Limits, modelling and design", *Proc. New Photovoltaics Materials for Solar Cells*, First Polish-Ukrainian Symposium, Cracow-Przegorzały, 58–78 (1996).
11. Z.T. Kuznicki, L. Wu, and S. Sidibé, "Multiinterface solar cells: II. Elements of realisation", *Proc. New Photovoltaics Materials for Solar Cells*, First Polish-Ukrainian Symposium, Cracow-Przegorzaly, 79–98 (1996).
12. Z.T. Kuznicki, "Multilayer and multiinterface structures for very high efficiency solar cells", *Proc.* SPIE, **3725**, 329–345 (1998).
13. U. Zammit, K.N. Madhusoodanan, M. Marinelli, F. Scudieri, F. Mercuri, E. Wendler, and W. Wesch, "Optical absorption in ion implanted Si films", *Nucl. Instr. Meth. Phys. Res.* **B 96**, 241–244 (1995).
14. L. Cspregi, E.F. Kennedy, T.J. Gallagher, and J.W. Mayer, "Recording of amorphous layers of Si implanted with $^{31}P^{+}$, ^{75}AS and ^{11}B ions", *J. Appl. Phys.* **48**, 4234 (1977)
15. Z.T. Kuznicki, I. Marton, R. Schindler, W. Wettling, and P. Holliger, "Some aspects of surface and interface defect activity", *2nd World Con. on Photovoltaic Solar Energy Conversion*, Vienna, 1407–1410 (1998).

